

## HYDRATE CELLULOSE FILMS AND PREPARATION OF FILM COMPOSITES WITH NICKEL NANO- AND MICROPARTICLES.

## I. PROPERTIES OF HYDRATE CELLULOSE FILMS

NINA E. KOTELNIKOVA and ALEXANDRA M. MIKHAILIDI\*

*Institute of Macromolecular Compounds, Russian Academy of Sciences, St. Petersburg, Russia**\*Saint-Petersburg State University of Technology and Design, St. Petersburg, Russia**Received March 22, 2011*

The properties and structure of a hydrate cellulose film have been studied by WAXS, FTIR spectroscopy, X-ray photoelectron spectroscopy, high-resolution  $^{13}\text{C}$  NMR spectroscopy in solid state, and scanning electron microscopy.

**Keywords:** hydrate cellulose film, properties, structure, physico-chemical analytical methods

**INTRODUCTION**

During the last decade, some effective methods to obtain and stabilize nanometer-sized metal particles embedded into various "hard" matrices (polymers, zeolites, etc.) have been developed. Materials containing metal nanoparticles evidence some unusual properties, such as giant magnetoresistance, an anomalously high magneto-caloric effect, etc. In the case of nanoparticles, the standard features of magnetic materials (saturation magnetization, coercive force, etc.) are usually not only equal, but often higher than similar parameters of the bulk materials.<sup>1-6</sup>

A research on the preparation of nanocomposites based on native insoluble polymer cellulose with metal nanoparticles intercalated into the cellulose matrix has been carried out.<sup>7</sup> Methods of embedding the nanoparticles of transition metals into the matrix of powdered microcrystalline cellulose (MCC) and in some other cellulosic materials have been developed. Nanocomposites of MCC and of metals, such as silver, copper, nickel and cobalt, have been obtained. In this case, the metals were in nanodispersed state, the nanocomposites possessing properties not inherent to cellulose. For example, the nanocomposites of MCC or of textile cellulose materials containing silver nanoparticles exhibited bac-

tericidal properties,<sup>8</sup> while the samples of MCC containing nickel and cobalt were ferromagnetic.<sup>9,10</sup> From a practical point of view, embedding of the metal particles into polymeric materials occurring as films,<sup>1,11</sup> is quite prospective. Film materials obtained from solutions of simple and complex ethers of cellulose are widespread.

The hydrate cellulose film (HCF), also named cellophane, obtained from the pulp of coniferous trees or cotton, is the only non-modified cellulose film and the most common low-cost packaging film material, largely consumed worldwide. HCFs are non-toxic, heat-resistant, have low vapor and water resistance, as well as high resistance to fats and micro-organisms.<sup>12-15</sup> To make films elastic, some plasticizers, mainly glycerol, are usually added to HCF during manufacturing. Due to the wide industrial production and demand manifested since 1960s, studies on the chemical and structural properties of HCFs were almost absent. Several articles, including patents, studied mainly the ways to impart some new properties to HCFs, for extending their application,<sup>16-20</sup> while the stability of HCFs to chemicals was less studied.

Currently, cellophane, due to the high cost of its manufacturing, is almost

substituted by the polypropylene film. HCFs are still used in membrane technologies, where high permeability in dry and wet state is required.

The usage of HCF in nanotechnological processes has been scarcely described, if considering mainly the intercalation of metal nanoparticles into HCF. There are some publications, mainly devoted to the obtaining of new materials with useful properties, yet no serious study of the processes can be mentioned. Thus, in some patents and papers, the preparation of packaging HCFs containing various additives including nanoparticles of silver or titanium dioxide with bactericidal properties, was described.<sup>16-20</sup> The process of film obtaining was accomplished by the inclusion of ready-made nanoparticles into the reaction mixture in its formation stage. HCF was first used<sup>8</sup> as a basis for nanocomposites with embedded silver nanoparticles in the form of clusters or aggregates. The silver nanoparticles were intercalated into the matrix by the reduction of silver ions to silver (0) directly in the film matrix. Tests on the antimicrobial activity of HCFs containing silver (0) in a nanodispersed state related to standard strains of several bacterial test cultures showed high antimicrobial activity. The inclusion of nanoparticles of transition metals in the HCFs has not been studied.

The aim of the present investigation has been to analyze the morphological and structural characteristics of the HCF that have not been described until now, and to study the modification of HCF by intercalation of nickel nanoparticles. The study is divided into 2 parts. In the former, the results obtained by X-ray photoelectron spectroscopy and scanning electron microscopy, providing new data to the study of HCF structure, are discussed. In the latter part, nickel species intercalation into the solid matrix of HCFs will be presented.

## EXPERIMENTAL

### Materials and procedure

A hydrate cellulose film produced by "Viscose" company (Russia) was used to study the morphological and structural characteristics, as well as a matrix for the inclusion of nickel particles. The main characteristics of the original HCFs are shown in Table 1. The content of glycerol in HCF was determined from the weight loss of the film, after repeated washings with distilled water and drying in vacuum at 40 °C. Thermal resistance was calculated from the

weight loss of HCFs during heating at temperatures ranging from 60 to 250 °C. The degree of HCF polymerization was determined by the viscosity of its solutions in a cadmium ethylenediamine complex.<sup>21</sup> The treatment of HCF with a nickel-ammonia complex  $[\text{Ni}(\text{NH}_3)_n]^{2+}$  ( $n = 5 - 6$ ) was performed for 30 min.<sup>9</sup> All reagents were of pure or analytical grade.

### Methods

Elemental analysis of the film was performed using a Hewlett Packard C, H, N-analyser, by a method described elsewhere.<sup>22</sup> The chemical content on the surface of the film was determined by X-ray photoelectron spectroscopy (XPS).

### Fourier transform infra-red spectroscopy

The chemical composition of the films was characterized on a Bruker ISF 88 FTIR spectrometer. The samples, measured in the reflection and transmission mode, were used in the form of films, as after milling. The powder samples were embedded into potassium bromide pellets (5 mg/100 mg KBr). The spectra resulting from measurements included 64 scans at a spectral resolution of 8  $\text{cm}^{-1}$ .

### <sup>13</sup>C NMR spectroscopy

The <sup>13</sup>C NMR high-resolution spectra in solid phase were recorded with a Bruker CXP-100 spectrometer, by rotating the samples at the "magic angle" of 54°7' and a frequency of 3.6 kHz. The operating frequency for the <sup>13</sup>C nuclei was of 25.16 MHz, and pulse channel duration <sup>13</sup>C = 1 ms. The repetition period of the pulse sequence was of 2.6 s. The number of storages ranged from 100 to 400. Cross-polarization and decoupling from protons was used. Chemical shifts were given in ppm, relative to the signal of tetramethylsilane.<sup>23,24</sup>

### X-ray photoelectron spectroscopy (XPS)

The XPS spectra were recorded on a PHI 5400 (Perkin-Elmer) electronic spectrometer with excitation by Mg radiation.<sup>14</sup> The samples were fixed on a standard holder and, after preliminary evacuation, were placed on a manipulator previously cooled with liquid nitrogen. A working vacuum not higher than 5.10<sup>-5</sup> torr was maintained. The chemical composition of the surface was determined from the overall spectra. The analysis of the chemical state of elements and the calculation of relative atomic concentrations were carried out from the spectra of individual photoelectron lines, with standard programs. The precision of binding energy ( $E_{\text{bound}}$ ) determination was of 0.1 eV, and that of quantitative analysis was of 10%. The spectra were calibrated by the C 1s line of hydrocarbon components with  $E_{\text{bond}} = 285.0$  eV (due to surface charging).<sup>24,25</sup>

**Wide-angle X-ray scattering (WAXS)**

The structure of HCFs was studied by wide-angle X-ray scattering on a DRON-2.0 diffractometer using  $\text{CuK}\alpha$  radiation. The X-ray

scattering intensity curves were registered in the scattering angle range  $5^\circ < 2\theta < 40^\circ$ , at an angle step of  $2\theta/\text{min}$ , and constant time (3 s).

Table 1  
Physico-chemical properties of HCF

Properties	Values		References
Density, $\text{g/cm}^3$	1.50-1.52		[12-15]
Hygroscopicity, %	12.8-13.9		“_”
Melting temperature till beginning of decomposition, $^\circ\text{C}$	175-205		“_”
Dielectric permeability at air relative humidity of 65 and frequency of 100 kHz	5.3		“_”
Stability to different impacts			
strong acids	bad		“_”
strong bases	bad		“_”
fats and oils	medium		“_”
organic solvents	good		“_”
Water-resistance (water uptake at high humidity for 24 h), %	45-115 (medium)		“_”
Stability to sunlight	good		“_”
Heat resistance, $^\circ\text{C}$	130		“_”
Frost resistance, $^\circ\text{C}$	-18		“_”
Thermostability (mass loss at heating) at T, $^\circ\text{C}$			Data of authors
	with glycerol	without glycerol	
60	5.9	2.8	“_”
90	10.3	2.3	“_”
120	11.7	2.4	“_”
180	15.2	3.4	“_”
250	21.5	7.8	“_”
Degree of polymerization	250		“_”
Content of elements and glycerol, %	glycerol	carbon	hydrogen
	13.0	39.8	6.7

**Scanning electron microscopy (SEM)**

The morphological structure of the films was characterized by scanning electron microscopy (SEM), on Stereoscan 360 (Cambridge, UK) and Jeol JSM-35 CF (Japan) electronic microscopes. The observation by Stereoscan 360 was accompanied by EDX analysis. The samples fixed on a carbon substrate in a special chamber were subjected to spraying in an inert atmosphere, using a gold target. The capture by Jeol JSM-35 CF, performed at 100-20000 magnifications and 15 kV voltage (on a Stereoscan 360) was carried out at a voltage of 20 kV. The histograms of the numerical distribution of nickel particles on the surface of samples according to their size were obtained by statistical processing of images, taking into account the diameter referring to the size of particles. For each sample, at least 500 particles were analyzed.

**RESULTS AND DISCUSSION**

The data listed in Table 1 show that the properties of HCF have been sufficiently detailed. However, their physico-chemical characteristics have been described in few

publications, no information being provided on the morphological structure of films. That is why, some physico-chemical properties and the morphological structure of HCF, involved in the chemical modification of HCF, have been approached in the present study. It was shown that some known characteristics of HCF do not coincide with the presented data. Thus, the thermal resistance of the films that did not contain glycerol, defined in the study by the weight loss during the heating of films, was significantly higher than that described in the literature.<sup>12-15</sup> For example, when heated to  $250^\circ\text{C}$ , HCF lost only 7.8% of its initial weight while, at lower temperatures, it was even more stable (Table 1).

As known, HCFs are chemically produced from native cellulose, but their elemental composition differs slightly from that of native cellulose. Thus, the contents of the main elements – carbon (39.8 wt%) and hydrogen (6.7 wt%) – are approximately

equal to those of the most chemically “pure” samples of cotton microcrystalline cellulose (44.4 wt% and 6.2 wt%, respectively). However, differences in the chemical composition of the native or regenerated cellulose samples and HCF could be ascertained by FTIR analysis and  $^{13}\text{C}$  NMR spectra.

#### Characterization of HCFs by FTIR, $^{13}\text{C}$ NMR and XPS methods

The comparison of the FTIR spectra of HCFs with the spectrum of either refined sulphate cellulose I (Fig. 1) or regenerated (mercerized) cellulose II revealed a great difference in the spectral ranges of 400-1800  $\text{cm}^{-1}$  and 2500-4000  $\text{cm}^{-1}$ . A typical spectrum of cellulose I contains absorption bands in the 3000-3600  $\text{cm}^{-1}$ , 2700-3000  $\text{cm}^{-1}$ , 1650  $\text{cm}^{-1}$ , 1300-1500  $\text{cm}^{-1}$  and 750-1200  $\text{cm}^{-1}$  ranges, which correspond to OH-stretching, aliphatic CH-stretching and bending modes, C=O, stretching of the CO ether bond of cellulose, and to the various peaks resulting from the glucopyranose ring of cellulose, respectively.<sup>26-28</sup> The shape of a broad absorption band of glucopyranose ring fluctuations in the 1000-1200  $\text{cm}^{-1}$  range of HCF, being a superposition of the absorption bands of CO and O-C-O groups, differed greatly from the same band in the spectrum of purified sulfate cellulose provided for comparison purposes.<sup>28</sup> The band in the HCF spectrum was narrower than that one in the spectrum of cellulose, and the intensity of the constituent bands was redistributed. In addition, the spectrum of the HCF absorption band at 910  $\text{cm}^{-1}$ , related to the antisymmetrical in-phase ring stretching vibrations, had a higher intensity than that in the spectrum of cellulose. The shape of the broad absorption band of the stretching vibrations of the OH groups in the 3000-3600  $\text{cm}^{-1}$  range, which is also a superposition of several absorption bands, reflecting the fluctuations of the OH groups included and not included in the hydrogen bonds, was also markedly different from the shape of the same band in the spectrum of cellulose. This absorption band in the spectrum of HCF was more symmetrical and was not divided into separate bands, which showed the commensurability of the number of OH groups included and not included in the H-bonds.

In the high-resolution  $^{13}\text{C}$  NMR spectrum of HCF in the solid state (Fig. 2), the basic

chemical shifts of the carbon atoms were within the areas with peaks at 62.4 ppm (chemical shifts of atoms  $\text{C}_6$ ), 83.1 ppm, 87.0 ppm (chemical shifts of atoms  $\text{C}_4$ ), and 104.7 ppm (chemical shifts of atoms  $\text{C}_1$ ), while the broad resonance of the  $\text{C}_{2,3,5}$  carbons in the 70-80 ppm range was not completely resolved or individually assigned. The positions of these peaks agreed with those described in the literature.<sup>25,28-31</sup> The comparison of the  $^{13}\text{C}$  NMR spectrum of HCF with the spectra of cellulose I and cellulose II, prepared by mercerization of cotton cellulose,<sup>25,30,31</sup> showed that the HCF spectrum was slightly different from that of cellulose II, while considerable differences appeared compared to the spectrum of cellulose I. Thus, the band of the chemical shifts of atoms  $\text{C}_{2,3,5}$ , with a maximum at 73.8 ppm, was not divided into two separate bands and was more symmetrical, which indicated a different conformation from that of cellulose I or from another molecular environment. In addition, the changes in the chemical shift of atoms  $\text{C}_6$  (62.9 ppm) towards the range with lower values indicated a change in the rotational-isomeric composition of the oxymethyl group. It should be also noted that HCF crystallinity, which could be estimated from the ratio of the intensity of chemical shifts of atoms  $\text{C}_4$ , 83.1 ppm and 87.0 ppm, as described in the literature,<sup>30,31</sup> was considerably lower than that of cellulose I and cellulose II.

The chemical composition of the HCF surface was evaluated by X-ray photoelectron spectroscopy (Fig. 3). As previously shown, the XPS spectrum of cellulose I, with deconvolution in the spectral region of carbon 1s line, contained 4 individual components with binding energies ( $E_{\text{bound}}$ ) corresponding to the carbon in groups C-H ( $E_{\text{bound}} = 285.0$  eV), C-OH and C-O-C ( $E_{\text{bound}} = 286.6$  eV), O-C-O and C = O ( $E_{\text{bound}} = 287.7$  eV) and carboxyl ( $E_{\text{bound}} = 289.1$  eV).<sup>24</sup> According to the spectra, the surface of cellulose I contains mostly hydroxyl, ether and carbonyl groups, also attended by a small number of carboxyl groups. In the XPS spectrum of the cellophane film,<sup>32</sup> a very intense C-O-C peak ( $E_{\text{bound}} = 286.7$  eV) appeared, accompanied by a small O-C-O peak ( $E_{\text{bound}} = 288$  eV) related to the cellulose structure. The presence of the C-H peak ( $E_{\text{bound}} = 284.7$  eV) was due to the impurities having emerged in the film during the manufacture process (Fig.

3, 1). When comparing the XPS spectra of cellulose I<sup>24,28,32</sup> and HCF (Fig. 3, 2), a great difference could be observed, while the XPS spectra of cellophane and HCFs seemed to be similar. Thus, in the HCF spectrum, an intense C-O-C peak with  $E_{\text{bound}} = 286.7$  eV was also present, however, the O-C-O peak ( $E_{\text{bound}} = 288$  eV) occurred as a shoulder,

with far less intensity than that recorded in the spectrum of cellophane. The HCF spectrum exhibited a significant difference, while the peak with  $E_{\text{bound}} = 285.0$  eV had a very low intensity, indicating the absence of organic impurities on the surface of HCF, *i.e.* its high chemical “purity”.

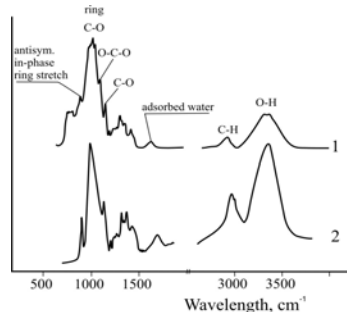


Figure 1: FTIR spectra of refined sulphate cellulose I (1)<sup>28</sup> and HCF (2)

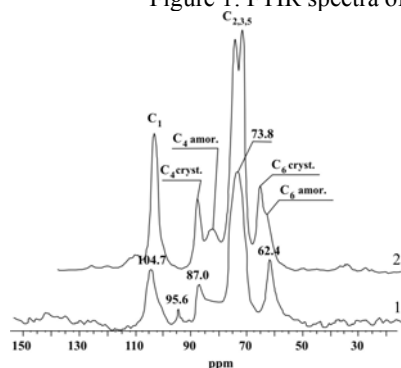


Figure 2: <sup>13</sup>C NMR spectra of HCF (1) and native cellulose I (2)

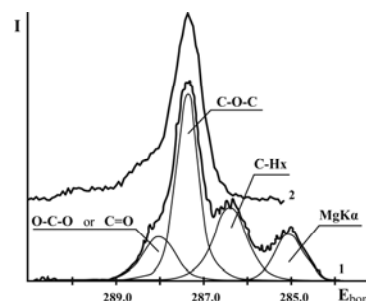


Figure 3: X-ray photoelectron spectra of cellophane (1)<sup>28,32</sup> and HCF (2)

### WAXS study

The supramolecular structure of HCF was quite different from that of native cellulose, which is the structure of cellulose I,<sup>32-35</sup> while the crystal structure of HCF could be identified as the structure of cellulose II (Fig. 4). However, the X-ray diffraction pattern of HCF did not totally correspond to the structure of cellulose II. Thus, the intense reflection in the  $2\theta$  20° range, which refers to the 020 reflection of the cellulose cells, was the only one in the studied range, since reflections at  $2\theta$  12° and 35°, both typical of cellulose II, were absent. This indicated that the supramolecular structure of HCF differed noticeably from that of the regenerated or mercerized cellulose, known as cellulose samples with the structure of cellulose II.

Numerous studies have shown that the X-ray crystallinity of cellulose II was considerably lower than that of cellulose I, therefore, in principle, cellulose II was more

chemically reactive.<sup>36</sup> This conclusion, mentioned in many publications, however, was not unique, since it did not consider some important characteristics of the cellulose samples, such as a capillary-porous structure and specific square of the pores. Cellulose is known to be a system of conjugate fibres consisting of fibrils. The developed capillary-porous structure of native cellulose samples includes nanopores, resulting from intrafibrillar packaging irregularity, with a size of about 1.5 nm; interfibrillar pores of 1.5-10 nm, occurring as a result of some internal strains (a few dozens of nm), as well as channels and pores with a diameter of a few  $\mu\text{m}$ . The above-mentioned features contribute to the high chemical reactivity of native cellulose, in spite of its quite high X-ray order. Reactivity remains also high for regenerated fibres, including the hydrate cellulose ones. Manufacturing of film materials by the

dissolution of native fibres, followed by subsequent regeneration and film formation, led to deformations in the fibrous structure of the samples and to serious changes in the capillary-porous structure. During chemical processes, when the pristine film is subjected to modification, it should be taken into account that HCF has a high density, of 1.50-1.52 g/cm<sup>3</sup> (Table 1),<sup>15</sup> which differs only a little from that of native fibres (1.54-1.56 g/cm<sup>3</sup>).<sup>15,37,38</sup> These properties, despite the low crystallinity of HCFs, can lead to some unexpected results, including the resistance of HCF to chemical impact. It should be also mentioned that a reliable determination of crystallinity for the cellulose samples that differ from the structure of cellulose I, is not sufficiently studied. Numerous calculations of crystallinity for cellulose with structural modifications II, III and IV, given in many publications, were mostly performed with formulas worked out for the estimation of the crystalline structure of cellulose I, which was not correct. Consequently, no calculated data on the crystallinity of HCF are presented here.

#### SEM study

Researches on the morphological structure of HCFs by SEM showed that the pristine film had a smooth, flat surface with parallel bands, apparently formed during film molding and extrusion. Film thickness was of ~30 μm, with morphologically different edges. There were significant layers at one edge with the top two layers thicker than the bottom ones, the top layers showing an amorphous morphology. Their total thickness was of 6.5-15 μm. Thickening and amorphization of the surface layer might be

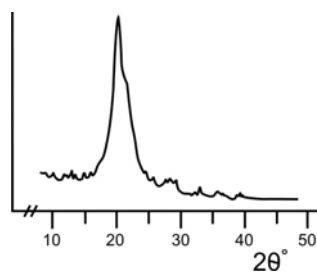


Figure 4: X-ray intensity curve of HCF

explained by the effect of the weak “melting” in the process of film formation. It could be assumed that, during chemical reactions, the above-mentioned structure of the surface layer would exert a barrier function and prevent penetration of chemicals into HCF. The other 6 layers were tightly molded parallel to the surface, having a total thickness of 15 μm (2.5 μm each) (Fig. 5.1).

The other edge had a clearly visible fibrillar structure. Fibrils were parallel to each other and were directed vertically to the film surface. The length of the fibrils was of 24-29 μm, the thickness of the fibrils was of 150-200 nm, and the distance among them was of 100-200 nm. The apparent disagreement of the arrangement of the layer, which was parallel to the film surface at one edge, and the structure of the parallel fibrils arranged vertically to the film surface at the other edge, could be explained as follows. The formation of such a structure was possible when each of the parallel layers from one edge formed by folded fibrils repeatedly stacked in the bulk of the film along its axis (*i.e.*, along the drawing direction of the film). Schematically, this is shown in Figure 5.2, drawn according to the scheme presented in the literature.<sup>39</sup> A similar structure has been established for the multilayer carbon nanotubes regularly coiled in the form of yarn along the axis of the material.

According to SEM data,<sup>40</sup> the crystallite length of hydrate cellulose fibres was of 15-85 nm, the range of values depending on the method of their manufacture.

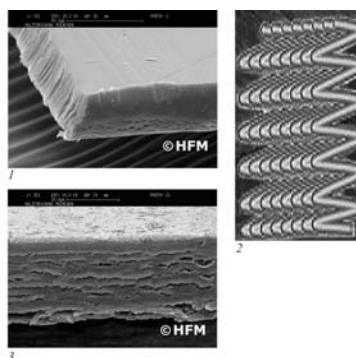


Figure 5: SEM of HCF surface and edges (1), schematic view of parallel layers formed folded along the axis in bulk of the film<sup>39</sup> (2), and HCF treated with [Ni(NH<sub>3</sub>)<sub>n</sub>]<sup>2+</sup> (3)

It could be assumed that the length of crystallites in the hydrate cellulose film was close to that of hydrate cellulose fibres. If the average length of the crystallites was accepted as equal to 50 nm, the calculations showed that each fibril consisted of 20-50 crystallites, while the thickness of fibrils corresponded to 3-4 crystallites. Thus, the SEM study of the original film showed that, morphologically, HCF was quite a complex formation. The morphology of its inner layers was highly ordered and the outer layers might perform a barrier function, which was probably determined by the manufacturing process. Therefore, despite the relatively low X-ray crystallinity, chemical reactions in the bulk of HCF, when used as a matrix for the penetration of chemicals or for the intercalation of micro- and nanoparticles of different types, could be hindered.

The chemical treatment of a film impacted considerably on its morphological structure. In the first stage of some diffusion-reduction processes, for instance, when the intercalation of nickel ions into HCF was performed, the film was treated with a solution of the nickel-ammonia complex  $[\text{Ni}(\text{NH}_3)_n]^{2+}$ . This treatment led to disturbances in the surface morphology and inner layers of the film. The film swelled in transverse direction, while its thickness markedly increased to 35-40  $\mu\text{m}$ . From the film edge, it could be seen that swelling of HCF was accompanied by layerwise separation of the swollen layers; after treatments, their thickness rose to 4.3-4.5  $\mu\text{m}$  (Fig. 5.3), and an increase of the interlayer space also occurred. Thus, the morphological structure of the pristine HCF characterized by high density and regular arrangement of the layers, under the impact of nickel-ammonia complex, became more labile, while its chemical accessibility was expected to increase.

**ACKNOWLEDGEMENTS:** We are grateful to A. Vieler (TU, Munich, Germany) for the assistance in sample observations with SEM, to Prof. G. Wegener (TU, Munich, Germany) for discussion, to A. V. Gribanov for recording high-resolution  $^{13}\text{C}$  NMR of HCF in solid state, to A. L. Shakhmin for recording the X-ray photoelectron spectra of the samples, to V. K. Lavrentiev for obtaining the X-ray intensity curve of HCF

and to E. N. Vlasova for recording the FTIR spectra of the samples.

## REFERENCES

- <sup>1</sup> A. Heimann, "Polymer Films with Embedded Metal Nanoparticles", Berlin, Heidelberg, Springer-Verlag, 2003, 216 pp.
- <sup>2</sup> S. P. Gubin, Yu. A. Koshkarov, G. B. Khomutov and G. U. Yurkov, *Usp. Khim.*, **74**, 539 (2005).
- <sup>3</sup> I. P. Suzdalev, *Usp. Khim.*, **78**, 267 (2009).
- <sup>4</sup> V. Yu. Doluda, S. V. Schennikov and N. V. Lakina, *Nanotekhnologii: Nauka i Proizvodstvo*, **1**, 4 (2009).
- <sup>5</sup> M. S. Li and S. I. Nam, Pat. 2259871 Ru (2005).
- <sup>6</sup> A. A. Revina, Pat. 2322327 Ru (2008).
- <sup>7</sup> N. Kotelnikova, U. Vainio, K. Pirkkalainen and R. Serimaa, *Macromol. Symp.*, **254**, 74 (2007).
- <sup>8</sup> N. E. Kotelnikova, O. V. Lashkevich and Ye. F. Panarin, Pat. 2256675 Ru (2005).
- <sup>9</sup> N. E. Kotelnikova, E. L. Lisenko, R. Serimaa, K. Pirkkalainen, U. Vainio, V. K. Lavrentiev, D. A. Medvedeva, A. L. Shakhmin, N. N. Saprikina and N. P. Novoselov, *Vysokomol. Soedin.*, series A, **49**, 1530 (2007).
- <sup>10</sup> K. Pirkkalainen, K. Leppanen, U. Vainio, T. Elbra, T. Kohout, A. Nykanen, N. E. Kotelnikova and R. Serimaa, *Eur. Phys. J.*, **49**, 333 (2008).
- <sup>11</sup> L. I. Trakhtenberg, G. N. Gerasimov, V. K. Potapov, T. N. Rostovschikova, V. V. Smirnov and V. Yu. Zufman, *Vestnik Mosk. Univ.*, series 2, **42**, 325 (2001).
- <sup>12</sup> P. V. Kozlov and G. I. Braginskiy, "Chemistry and Technology of Polymer Films", (in Russian), Moscow, Iskusstvo, 1965, 624 pp.
- <sup>13</sup> Z. A. Rogovin, "Fundamentals of Chemistry and Technology of Chemical Fibres Production", (in Russian), Moscow, Mir, 1964, 642 pp.
- <sup>14</sup> Z. A. Rogovin and L. S. Galbraikh, "Chemical Transformations and Modification of Cellulose", (in Russian), Moscow, Khimia, 1979, 206 pp.
- <sup>15</sup> A. B. Pakshver (Ed.), "Properties and Processing Characteristics of Chemical Fibres", (in Russian), Moscow, Khimia, 1975, 495 pp.
- <sup>16</sup> M. Koenig, V. Effern, S. Redmann-Schmid and W. Lutz, Pat. 20080145576 USA (2008).
- <sup>17</sup> <http://polymers-money.com/journal/onlinejournal/2005/>
- <sup>18</sup> E. Kontturi, T. Tammelin and M. Osterberg, *Chem. Soc. Rev.*, **35**, 1287 (2006).
- <sup>19</sup> E. Kontturi, P. C. Thune and J. W. Niemantsverdriet, *Langmuir*, **19**, 5735 (2003).
- <sup>20</sup> T. P. Starunskaya, *PhD Thesis*, Leningrad, 1984, 142 p.
- <sup>21</sup> L. S. Bolotnikova, S. N. Danilov and T. I. Samsonova, *Zh. Prikl. Khim.*, **39**, 176 (1966).
- <sup>22</sup> V. A. Klimova, "The Main Micro-Analysis of Organic Compounds", (in Russian), Moscow, Khimia, 1975, 224 pp.
- <sup>23</sup> N. E. Kotelnikova, A. Yu. Elkin, A. I. Koltsov, G. A. Peyropavlovskiy and Yu. N. Sazanov, in

“Methods of Cellulose Research”, edited by V. P. Karlivan, Riga, Zinatne, 1988, pp. 61-63.

<sup>24</sup> N. E. Kotelnikova, G. Wegener, T. Paakkari, R. Serimaa, E. Windeisen, H. Knozinger, M. Scheithauer, V. N. Demidov, A. V. Shchukarev and A. V. Gribanov, *Cellulose Chem. Technol.*, **36**, 445 (2002).

<sup>25</sup> A. V. Shukarev, S. A. Dobrusina and V. I. Sukharevich, *Zh. Prikl. Khim.*, **68**, 1680 (1995).

<sup>26</sup> D. Fengel, *Holzforschung*, **46**, 283 (1992).

<sup>27</sup> D. Fengel, M. Ludwig and M. Przyklenk, *Das Papier*, **7**, 323 (1992).

<sup>28</sup> E. J. Konturri, *Academic Dissertation*, Eindhoven, 2005, 145 p.

<sup>29</sup> J. Zawadzki and M. Wisniewski, *J. Anal. Appl. Pyrol.*, **62**, 111 (2002).

<sup>30</sup> J. C. Gast, R. H. Atalla and R. D. McKelvey, *IPC Technical Paper Series*, **86**, 1 (1979).

<sup>31</sup> S.-L. Maunu, T. Liitia, S. Kauliomaki, B. Hortling and J. Sundquist, *Cellulose*, **7**, 147 (2000).

<sup>32</sup> F. Denes, R. Sitaru and R. A. Young, *J. Photopolym. Sci. Tech.*, **11**, 299 (1998).

<sup>33</sup> N. M. Bikales and L. Segal (Eds.), “Cellulose and Cellulose Derivatives”, New York, Wiley-Interscience, 1971, 718 pp.

<sup>34</sup> F. J. Kolpak and J. Blackwell, *Macromolecules*, **9**, 273 (1976).

<sup>35</sup> F. J. Kolpak and J. Blackwell, *Text. Res. J.*, **48**, 458 (1978).

<sup>36</sup> L. M. Kroon-Batenburg and J. Kroon, *Glycoconjugate J.*, **14**, 677 (1997).

<sup>37</sup> Z. A. Rogovin, “Chemistry of Cellulose”, (in Russian), Moscow, Khimia, 1972, 520 pp.

<sup>38</sup> D. Fengel and G. Wegener, “Wood. Chemistry, Ultrastructure, Reactions”, Berlin – N.Y., Walter de Gruyter, 1989, 613 pp.

<sup>39</sup> [http: www.strf.ru/science.aspx](http://www.strf.ru/science.aspx)

<sup>40</sup> [http: www.chemport.ru/chemical\\_encyclopedia\\_article\\_2064.html](http://www.chemport.ru/chemical_encyclopedia_article_2064.html)